Observation of Interactions between Trapped Ions and Ultracold Rydberg Atoms

N. V. Ewald, T. Feldker, H. Hirzler, H. A. Fürst, and R. Gerritsma

Van der Waals-Zeeman Institute, Institute of Physics, University of Amsterdam, 1098 XH Amsterdam, the Netherlands

We report on the observation of interactions between ultracold Rydberg atoms and ions in a Paul trap. The rate of observed inelastic collisions, which manifest themselves as charge transfer between the Rydberg atoms and ions, exceeds that of Langevin collisions for ground state atoms by about 3 orders of magnitude. This indicates a huge increase in interaction strength. We study the effect of the vacant Paul trap's electric fields on the Rydberg excitation spectra. To quantitatively describe the exhibited shape of the ion loss spectra, we need to include the ion-induced Stark shift on the Rydberg atoms. Furthermore, we demonstrate Rydberg excitation on a dipole-forbidden transition with the aid of the electric field of a single trapped ion. Our results confirm that interactions between ultracold atoms and trapped ions can be controlled by laser coupling to Rydberg states. Adding dynamic Rydberg dressing may allow for the creation of spin-spin interactions between atoms and ions, and the elimination of collisional heating due to ionic micromotion in atom-ion mixtures.

Introduction.—On ultracold neutral atoms, Rydberg excitation has been employed to engineer both the interaction strength and range [1–6]. The resulting long-range interactions find applications in studying quantum many-body physics [7] and in quantum information processing [8]. In the same spirit, it has been proposed to control the interactions between atoms and trapped ions by coupling the atoms to Rydberg states [9–11]. Since the polarizability of Rydberg atoms scales with the principle quantum number n to the power of seven, the charge-induced dipole interactions between atoms and ions are orders of magnitude larger for Rydberg-coupled atoms, and the range over which the interactions are relevant can extend over tens of micrometers. Furthermore, Rydberg dressing may allow tuning the polarizability of the atoms without losses due to the finite lifetime of Rydberg states, in analogy to schemes in neutral atoms [12–17]. Dynamic control over the Rydberg-dressed atom-ion system would allow for the creation of atom-ion spin-spin interactions [10] and tailoring of repulsive atom-ion interactions. The latter suppresses micromotion-induced heating [11] which has formed the major limitation in creating ultracold atom-ion mixtures [18,19].

In this Letter, we report on the observation of interactions between single ^{174}Yb$^+$ ions in a Paul trap and a gas of ultracold ^{6}Li atoms excited to the Rydberg states $24S$ and $24P$. We study the effect of the vacant Paul trap by observing atom loss after Rydberg excitation. We fit the observed loss spectrum with a model taking into account the independently measured electric fields of the Paul trap. By juxtaposing the number of trapped ions counted before and after Rydberg excitation in the hybrid trap's center, we

obtain an ion loss rate. We identify the ion loss with charge transfer following an inelastic collision between a Rydberg atom and an ion. Comparing this loss rate to the one of ground state atoms colliding with ions in the $^2D_{3/2}$ state—for which we measured the charge exchange rate before [20]—we infer an ion loss rate that is at least $1.1(4) \times 10^3$ times higher than the Langevin collision rate of ground state atoms. This indicates a huge increase in interaction strength. We fit the spectral shape of the ion loss with a classical model of colliding Rydberg atoms and ions, taking into account the finite lifetime of the Rydberg state and the Rydberg atoms' Stark shift induced by the electric fields of both the ion trap and the trapped ion. Finally, we excite the atoms to the Rydberg state $24P$ via a dipole-forbidden transition. We explain these results by the admixing of the nearby $24D$ state due to the intense electric field of the ion in its vicinity, such that the transition to the Stark-shifted state becomes allowed.

Setup and procedure.—Details on our experimental setup can be found in Refs. [20,21]. In short, we prepare a cloud of ^{6}Li atoms in a magneto-optical trap (MOT) about 20 mm below the center of our Paul trap, magnetically compress and transport it there, and apply a second MOT stage to increase its phase space density. Next, the atoms are optically pumped into an equal spin mixture of the ground state's lower hyperfine manifold $|2^2S_{1/2}, F = 1/2\rangle$, and loaded into a crossed optical dipole trap (ODT), as sketched in Fig. 1(a). To perform forced evaporative cooling, we increase the scattering length between atoms in the two magnetic hyperfine levels by applying a magnetic field of 663G [22,23]. We evaporate the atoms down to a temperature of $T \approx 15~\mu$K in about 1.5 s by
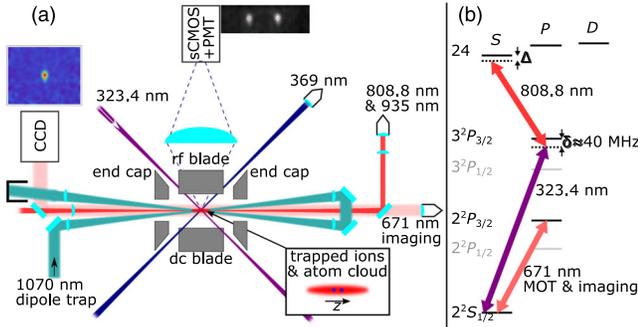
FIG. 1. Overview of the experiment. (a) Sketch of the setup. The ions are trapped in a Paul trap (gray) consisting of four blade electrodes and two end caps, where they are Doppler cooled with light at 369 nm (blue). A repumper at 935 nm (red) prevents population trapping in a metastable state. We image the ions' fluorescence onto an sCMOS camera and a photomultiplier tube (PMT). The atoms are trapped in a crossed-beam optical dipole trap (turquoise) at 1070 nm, which we shine into the ion trap through apertures in its end caps. We detect the atoms by absorption imaging with resonant light at 671 nm (light red). (b) Simplified level scheme of ^{6}Li. We populate the Rydberg state 24S (and later 24P) by two-photon excitation via the intermediate $3^2P_{3/2}$ state. The light at 323.4 nm (violet) is detuned from the $2^2S_{1/2} \to 3^2P_{3/2}$ transition by about $\delta \approx 40(10)$ MHz, while the 808.8 nm laser (red) is scanned over the Rydberg resonances (Δ).

lowering the laser power of the ODT, ending up with up to $N_{\text{atom}} \approx 10^5$ atoms at a peak density of $\rho = N_{\text{atom}}/[(2\pi)^{3/2}\sigma_x\sigma_y\sigma_z] \approx 10^5/[(2\pi)^{3/2}21\times47\times250]\,\mu m^{-3} \approx 2.6\times10^{16}$ m^{-3}, σ_i being the Gaussian widths in the respective direction. The cigar-shaped atom cloud is imaged along the common trap axis z.

As depicted in Fig. 1(b), we perform two-photon Rydberg excitation of ^{6}Li to the 24S state via the intermediate $3^2P_{3/2}$ state from which we red detune by $\delta \approx 40(10)$ MHz. To achieve this, laser pulses at 323.4 and 808.8 nm are applied while the ODT and all magnetic fields are switched off. The two-photon Rabi frequency $\Omega_{\text{eff}} \approx \Omega_{323.4}\Omega_{808.8}/(2\delta)$ is on the order of 1 MHz. In order to perform spin-selective detection of the atoms, we subsequently switch the magnetic field to 767 G. Rydberg excitation is observed as a loss of atoms in the upper spin state of the ground state's lower hyperfine manifold, $|2^2S_{1/2}, F=1/2, m_F=-1/2\rangle$, probed by absorption imaging on the $2^2S_{1/2} \to 2^2P_{3/2}$ transition. We scan the frequency of the second excitation laser at 808.8 nm around the Rydberg levels to obtain the spectra as functions of the two-photon detuning Δ.

We trap one to three ^{174}Yb$^+$ ions in our Paul trap, operated at a radio frequency (rf) trap-drive frequency of $\Omega_{\text{rf}} = 2\pi \times 1.05$ MHz. The dynamic stability parameters $q = 0.13(0.27)$ correspond to trap frequencies of $\omega_x \approx \omega_y \approx 2\pi \times 48(100)$ kHz and $\omega_z \approx 2\pi \times 13(27)$ kHz, respectively. We observe fluorescence by driving the
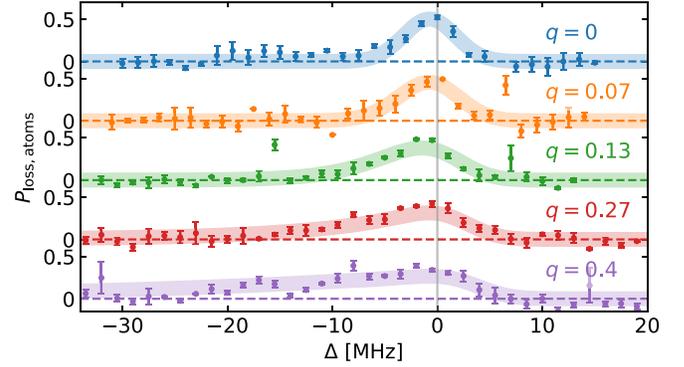

FIG. 2. Effect of the Paul trap field on the Rydberg spectra of 24S. We measure relative atom loss following Rydberg excitation at different stability parameters $q \in [0, 0.4]$. From $q = 0.13$ on, we see a modest asymmetric increase in resonance width. The results agree with numerical simulations (shaded lines), assuming a radial size of the atom cloud of $\sigma_r = 25\,\mu m$.

$^2S_{1/2} \to {}^2P_{1/2}$ Doppler cooling transition at 369 nm. To quantify the ion loss due to charge transfer, we count the number of ions before and after the interaction with the Rydberg-excited atoms by imaging them onto an sCMOS camera, as illustrated in Fig. 1(a). We overlap atoms and ions by maximizing the ion loss rate of ions excited to the $^2P_{1/2}$ state colliding with ground state atoms.

Results.—Before performing hybrid Rydberg atom-ion experiments, the effect of the electric ion trapping field on the Rydberg excitation has to be explored. This field is given by $\vec{E}_{\text{PT}}(\vec{r}, t) = (\nabla E_{\text{rf}})_r \cos(\Omega_{\text{rf}}t)(x, -y, 0)^T + \vec{E}_s(\vec{r})$, with $\vec{r} = (x, y, z)^T$ the position of the ion, and $(\nabla E_{\text{rf}})_r = mq\Omega_{\text{rf}}^2/(2e)$, with m the mass and e the charge of the ion. Note that the ion trap's static field $\vec{E}_s(\vec{r})$ is much smaller than the time-dependent rf field, and vanishes completely at the location of the ion, making it negligible. We change the radial rf electric field gradient of the vacant Paul trap, $(\nabla E_{\text{rf}})_r \approx q \times 3.9 \times 10^7$ V m^{-2} [24], and observe the line shape of the Rydberg loss spectrum as presented in Fig. 2. Note that we achieve stable ion trapping for a stability parameter $q \gtrsim 0.1$. We fit the spectra with a model (described in detail below) which includes the effects of the dynamic trapping field on the Rydberg state, convolved with the minimum width, $q = 0$ in Fig. 2, due to laser frequency fluctuations, Doppler broadening from thermal velocity distribution and Zeeman broadening from residual magnetic fields. The weaker van der Waals Rydberg-Rydberg interaction amounting to $C_6\rho^2/h \sim$ 50 kHz, with C_6 the dispersion coefficient [25,26] and h Planck's constant, can be neglected. Our model is in good agreement with the experimental results. Operating the trap using low trapping voltages $q \lesssim 0.1$, the aforementioned broadening effects dominate the observed linewidths. For larger trap drive amplitudes up to $q = 0.4$, an asymmetric and broad, albeit clear, resonance is visible. The increase of its red-side flank is predominantly attributed to the ion
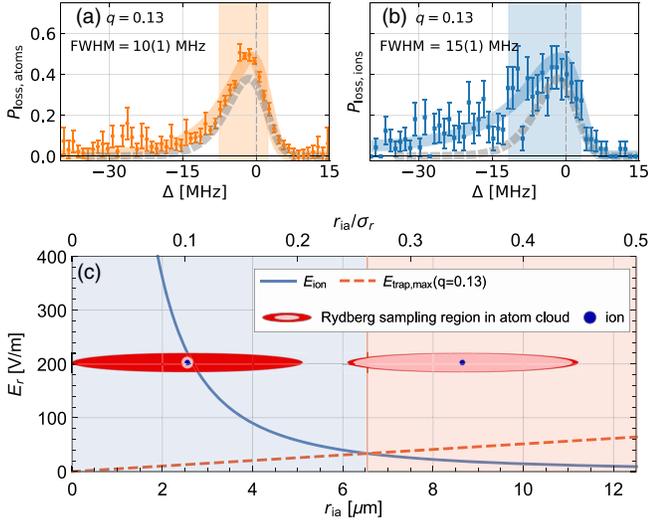
FIG. 3.   Rydberg excitation of ultracold atoms and collisions with trapped ions. (a) Atom and (b) ion loss probability Stark spectra after Rydberg excitation to $24S$. The spectra are obtained by averaging 19 up to 22 frequency scans. The presented model (shaded lines) fits the data and the colored bars indicate the full width at half maximum. The shape and width of the atom loss spectrum in the vacant Paul trap (grey dashed) are comparable to the atom loss, but the ion loss spectrum exhibits a long spectral tail on the resonance's red side, which can be explained by including the ion-induced Stark shift. (c) Comparison of radial electric field amplitudes of an ion and the trap's rf amplitude for $q = 0.13$. The two graphics depict the ion (blue) immersed in the atom cloud (red) with the two respective sampling regions of detectable Rydberg excitation (light red). An ion probes charge transfer with a single nearby Rydberg-excited atom (left), whereas atom loss due to Rydberg excitation occurs throughout the whole cloud (right).

trap's Stark shift on the Rydberg state [25], which has a polarizability of $\alpha_{24S} = 3.1 \times 10^6$ Hz/(V^2/cm^2) that is a factor 7.6×10^7 larger than that of the ground state [27]. We conclude that simultaneous trapping of ^{174}Yb$^+$ ions and Rydberg excitation of ^{6}Li atoms is feasible.

We now perform the experiment with ions loaded into the trap, for which we set $q = 0.13$ and apply a laser pulse of length $T_{\text{pulse}} \approx 20$ μs to excite the atoms to $24S$. Subsequent atom loss globally samples Rydberg excitation because of wide laser foci spanning the whole cloud. The atom loss spectrum shown in Fig. 3(a) exhibits a similar shape and width as compared to the corresponding case without ions in Fig. 2 ($q = 0.13$, green). Note that the slightly higher probability is due to higher saturation of the transition due to higher laser powers.

Simultaneously, we are able to independently measure ion loss after the interaction time. The long-range interaction potential between an ion and a Rydberg atom in an $n^2 S_{1/2}$ state has the form $V_{\text{ia}} = -C_4^{nS}/(2r_{\text{ia}}^4)$, for large atom-ion distances r_{ia} [9,10]. Here, C_4^{nS} is the coefficient for charge-induced dipole interaction, proportional to the

atom's scalar polarizability α_{nS}. At closer range, the potential becomes more complex as many avoided crossings between energy surfaces occur [10], leading to inelastic processes such as charge transfer [28,29]. A simple classical over-barrier model of ion-Rydberg atom collisions predicts a charge transfer probability of $P_{\text{ct}} = 0.5$ per collision, because the relative velocity of the Rydberg atom-ion system is much smaller than the velocity of the Rydberg electron, such that its final position gets randomized [28]. As the ^{6}Li$^+$ ion is too light, it won't be trapped, since $q_{\text{Li}} \approx 7.8$ such that it is not contained in the stability region of the Paul trap [24].

The saturated ion loss probability spectrum shown in Fig. 3(b) reveals a long tail on the resonance's red side. The full width at half maximum (FWHM, colored bars) increase from 10(1) MHz in the atom loss to 15(1) MHz in the ion loss spectrum. The ion loss probability does not approach unity, most likely because a single collision can send the ion into an orbit beyond the atom cloud, suppressing further ones. Both the trapped ion and ion trap contribute to the Stark effect the charge-transferring atom experiences when Rydberg excited, manifesting itself as the observed red-sided broadening. The deviation from the reference atom loss case (grey dashed) likely stems from the Coulomb field of a centered ion which dominates the radial rf trap field amplitude over a distance of about 6.5 μm, indicated by the blue region in Fig. 3(c). Only Rydberg atoms excited within this region should contribute to the ion loss signal, since atoms excited in the trap-dominated region (orange) are accelerated away by the trap. This suggests that the ion loss spectrum is wider due to the intense electric field of the ion, which cannot be resolved in the atom loss spectra by absorption imaging since on average only about 10 out of 10^5 atoms reside in each ion-dominated electric field region.

The model to be convolved and fit to the data is simulated using a Monte Carlo method to sample atomic starting conditions. We then calculate the atoms' Stark shift, and thus Rydberg excitation frequency shift Δ, accounting for all electric fields. To model the ion loss spectra, the sampled starting conditions are propagated dynamically under the influence of all electric fields. We assume that the ion is initially trapped in the center, where the trap's fields are naturally zero. Charge transfer can occur once the distance between the atom and ion falls below $r_{\text{min}} = 200$ nm, corresponding roughly to the distance where the potential barrier between atom and ion opens for the $24S$ state [28]. We weight the obtained collision probabilities with the lifetime of the Rydberg atoms of about $\tau_{24S} \approx 11$ μs [25], within which they can travel a few micrometers; i.e., we probabilistically dismiss the cases where the atom does not make it to the ion. From the simulation of 10^7 randomly sampled atomic starting conditions, we obtain a relative collision rate $\nu_{\text{rel}}(\Delta)$, determining the spectral shape. We calculate the ion loss

probability during the Rydberg excitation pulse according to Poissonian statistics as $P_{\text{loss}} = P_{\text{ct}}(1 - e^{-\nu_{\text{rel}}(\Delta) \cdot s})$, where the saturation parameter s depends on N_{atom}, Ω_{eff}, and T_{pulse}. All parameters other than the only fit parameter s are obtained from the model or independent measurements. Further details on the simulation [30,31] and fitting are given in the Supplemental Material [32].

To prove the enhancement of the atom-ion interaction strength by Rydberg excitation, we compare the ion loss rate of ions colliding with atoms excited to the $24S$ state, Γ_{24S}, to the Langevin collision rate of ground state atoms. To obtain the latter, we measure the charge transfer rate of ground state atoms colliding with ions in the metastable $^2D_{3/2}$ state, Γ_D, accounting for the charge transfer probabilities. In this measurement, we omit the Rydberg laser pulse and use the 369 nm laser to pump the ions to the $^2D_{3/2}$ state. We alternate four times between the measurement with resonantly excited Rydberg atoms and the reference measurement in sets of each about 100 repetitions for interaction times of 20 μs (50 ms) and lost 173(96) out of 561(557) ions in total, respectively. From this, we obtain averaged ion loss rates and then a ratio of $\Gamma_{24S}/(P_{\text{ct}}\Gamma_D) = 18(2) \times 10^3$. The charge transfer rate of the $^2D_{3/2}$ state was determined to be 0.030(11) per Langevin collision [20]. Assuming that the average probability for the atoms to be in the Rydberg state is $P_{\text{Ryd}} \leq 0.5$, we conclude that the Rydberg atom-ion collision rate exceeds the Langevin collision rate of ground state atoms by at least a factor of $1.1(4) \times 10^3$.

Finally, we study Rydberg excitation to the $24P$ state, which is dipole forbidden in our two-photon excitation scheme. However, the electric field of a trapped ion Stark mixes the $24P$ state with the nearby $24D$ state such that excitation becomes allowed close to the ion [11]. To ensure that the ions do not venture into high-field regions [cf. Fig. 3(a)] before the Rydberg excitation pulse, we observe the ions' fluorescence at a position outside of the atom cloud before shuttling them inside it. This allows us to discard instances where the ions were not cooled into the trap center before the excitation pulse. Independent Monte Carlo simulations (blue shaded line) take the Stark admixing into account by scaling the Rydberg excitation probability with the square of the local electric field. A saturation parameter s and frequency offset Δ_0 are the only fit parameters. Further details can be found in the Supplemental Material [32].

We measure ion loss using a long excitation pulse of 500 μs and maximal laser power, presented in Fig. 4(a). A clear ion loss signal (blue, squares) at the expected excitation frequency is detected. The gray shaded region around $\Delta = 0$ indicates the calculated value of the two-photon resonance frequency to the bare $24P$ state and the uncertainty due to our wavelength meter. The displayed ion loss background measurement (gray, diamonds) is taken without atoms getting excited by blocking the first-step Rydberg laser. Without having loaded atoms into the trap but lasers on, we do not detect a single ion getting lost (gray
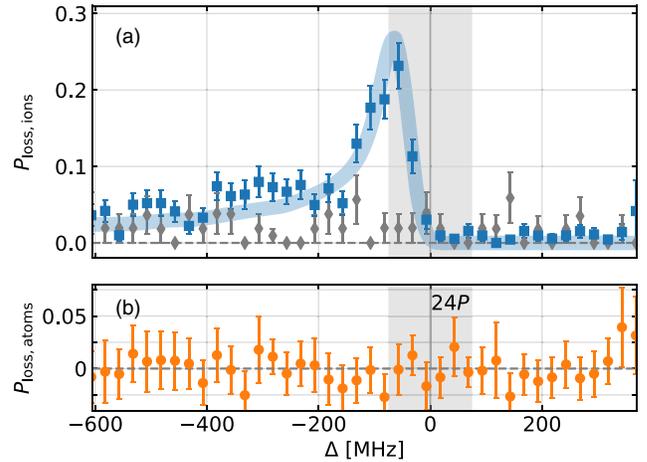

FIG. 4. Dipole-forbidden Rydberg excitation to $24P$ with the aid of the electric field of a single ion. (a) Ion loss probability due to charge transfer with Rydberg atoms is clearly detected (blue, squares). For comparison, background ion loss (first-step Rydberg laser switched off) is also shown (gray, diamonds). (b) No significant atom loss can be observed, because the fraction of atoms being close to the ion and thus able to be excited is small. The spectra are obtained by averaging about 90 frequency scans.

abscissa). Both arguments confirm the fact that the observed ion loss is a consequence of Rydberg atom-ion interaction. In contrast, we do not observe any significant atom loss signal as depicted in Fig. 4(b), since most atoms are far away from the ion and thus cannot be excited to the $24P$ state. The large redshift is caused by the about 10 times higher polarizability of the $24P$ state, its nonresolved fine structure, and the fact that significant Stark admixing of the D state demands intense electric fields. Therefore, we conclude that we have enabled Rydberg excitation on a dipole-forbidden transition with the aid of the electric field of a single trapped ion via Stark mixing.

Summary.—(i) We merged Rydberg excitation of ultracold atoms with ions in a Paul trap. (ii) We demonstrated the enhancement of atom-ion interactions by coupling to Rydberg states. (iii) We modeled the asymmetric Stark broadening due to ion and ion trap. (iv) We Rydberg-excited atoms on a dipole-forbidden transition with the aid of the electric field of a single trapped ion.

Outlook.—Our results point the way to experiments where atoms are laser dressed with Rydberg states with full dynamic control, letting us combine large and tunable atom-ion interactions with long lifetimes, and not suffering charge transfer. Possible applications may be the generation of entanglement or spin-spin interactions between ions and atoms [10]. Moreover, Rydberg couplings on dipole-forbidden transitions form a key ingredient in proposed schemes to suppress micromotion-induced heating [11,33]. In particular, repulsive atom-ion interactions could be created by dressing on such transitions. The implementation of these schemes requires a lower starting temperature of the mixture, and a single-step Rydberg-coupling scheme to create sufficiently high repulsive barriers,

[1] D. Jaksch, J. I. Cirac, P. Zoller, S. L. Rolston, R. Côté, and M. D. Lukin, Phys. Rev. Lett. **85,** 2208 (2000).
[2] R. Heidemann, U. Raitzsch, V. Bendkowsky, B. Butscher, R. Löw, L. Santos, and T. Pfau, Phys. Rev. Lett. **99,** 163601 (2007).
[3] A. Reinhard, K. C. Younge, T. C. Liebisch, B. Knuffman, P. R. Berman, and G. Raithel, Phys. Rev. Lett. **100,** 233201 (2008).
[4] M. Reetz-Lamour, T. Amthor, J. Deiglmayr, and M. Weidemüller, Phys. Rev. Lett. **100,** 253001 (2008).
[5] T. F. Gallagher and P. Pillet, Adv. At., Mol., Opt. Phys. **56,** 161 (2008).
[6] M. Saffman, T. G. Walker, and K. Mølmer, Rev. Mod. Phys. **82,** 2313 (2010).
[7] H. Bernien, S. Schwartz, A. Keesling, H. Levine, A. Omran, H. Pichler, S. Choi, A. S. Zibrov, M. Endres, M. Greiner, V. Vuletić, and M. D. Lukin, Nature (London) **551,** 579 (2017).
[8] D. S. Weiss and M. Saffman, Phys. Today **70,** No. 7, 44 (2017).
[9] Y. Hahn, Phys. Rev. A **62,** 042703 (2000).
[10] T. Secker, R. Gerritsma, A. W. Glaetzle, and A. Negretti, Phys. Rev. A **94,** 013420 (2016).
[11] T. Secker, N. Ewald, J. Joger, H. Fürst, T. Feldker, and R. Gerritsma, Phys. Rev. Lett. **118,** 263201 (2017).
[12] N. Henkel, R. Nath, and T. Pohl, Phys. Rev. Lett. **104,** 195302 (2010).
[13] G. Pupillo, A. Micheli, M. Boninsegni, I. Lesanovsky, and P. Zoller, Phys. Rev. Lett. **104,** 223002 (2010).
[14] F. Maucher, N. Henkel, M. Saffman, W. Krolikowski, S. Skupin, and T. Pohl, Phys. Rev. Lett. **106,** 170401 (2011).
[15] J. B. Balewski, A. T. Krupp, A. Gaj, S. Hofferberth, R. Löw, and T. Pfau, New J. Phys. **16,** 063012 (2014).
[16] Y.-Y. Jau, A. M. Hankin, T. Keating, I. H. Deutsch, and G. W. Biedermann, Nat. Phys. **12,** 71 (2016).

[17] J. Zeiher, R. van Bijnen, P. Schauß, S. Hild, J.-Y. Choi, T. Pohl, I. Bloch, and C. Gross, Nat. Phys. **12,** 1095 (2016).
[18] M. Cetina, A. T. Grier, and V. Vuletić, Phys. Rev. Lett. **109,** 253201 (2012).
[19] Z. Meir, M. Pinkas, T. Sikorsky, R. Ben-shlomi, N. Akerman, and R. Ozeri, Phys. Rev. Lett. **121,** 053402 (2018).
[20] J. Joger, H. Fürst, N. Ewald, T. Feldker, M. Tomza, and R. Gerritsma, Phys. Rev. A **96,** 030703(R) (2017).
[21] H. Fürst, T. Feldker, N. V. Ewald, J. Joger, M. Tomza, and R. Gerritsma, Phys. Rev. A **98,** 012713 (2018).
[22] F. Schreck, G. Ferrari, K. L. Corwin, J. Cubizolles, L. Khaykovich, M.-O. Mewes, and C. Salomon, Phys. Rev. A **64,** 011402(R) (2001).
[23] C. Chin, R. Grimm, P. S. Julienne, and E. Tiesinga, Rev. Mod. Phys. **82,** 1225 (2010).
[24] D. Leibfried, R. Blatt, C. Monroe, and D. Wineland, Rev. Mod. Phys. **75,** 281 (2003), Note that the implicit continued fractions which solve the recursive sequences of the trapped ion's Mathieu equations using Floquet theorem to obtain the motional harmonic approximation implicitly given here, deviate.
[25] N. Šibalić, J. D. Pritchard, C. S. Adams, and K. J. Weatherill, Comput. Phys. Commun. **220,** 319 (2017).
[26] N. Šibalić, J. D. Pritchard, C. S. Adams, and K. J. Weatherill, Comput. Phys. Commun., **220,** 319 (2017).
[27] A. A. Kamenski and V. D. Ovsiannikov, J. Phys. B **47,** 095002 (2014).
[28] V. N. Ostrovsky, J. Phys. B **28,** 3901 (1995).
[29] D. Vrinceanu and M. R. Flannery, Phys. Rev. Lett. **85,** 4880 (2000).
[30] H. Fürst, N. V. Ewald, T. Secker, J. Joger, T. Feldker, and R. Gerritsma, J. Phys. B **51,** 195001 (2018).
[31] H. A. Fürst, Ph. D. thesis, 2018.
[32] See Supplemental Material at http://link.aps.org/supplemental/10.1103/PhysRevLett.122.253401 for details on the numerical simulations and justification measurements, Refs. [25,28,30,31].
[33] L. Wang, M. Deiß, G. Raithel, and J. Hecker Denschlag, arXiv:1901.08781.
[34] M. Krych and Z. Idziaszek, Phys. Rev. A **91,** 023430 (2015).
[35] Z. Meir, T. Sikorsky, R. Ben-shlomi, N. Akerman, Y. Dallal, and R. Ozeri, Phys. Rev. Lett. **117,** 243401 (2016).
[36] M. Tomza, K. Jachymski, R. Gerritsma, A. Negretti, T. Calarco, Z. Idziaszek, and P. S. Julienne, arXiv:1708.07832.
[37] C. Kollath, M. Köhl, and T. Giamarchi, Phys. Rev. A **76,** 063602 (2007).
[38] H. Doerk, Z. Idziaszek, and T. Calarco, Phys. Rev. A **81,** 012708 (2010).
[39] U. Bissbort, D. Cocks, A. Negretti, Z. Idziaszek, T. Calarco, F. Schmidt-Kaler, W. Hofstetter, and R. Gerritsma, Phys. Rev. Lett. **111,** 080501 (2013).
[40] K. S. Kleinbach, F. Engel, T. Dieterle, R. Löw, T. Pfau, and F. Meinert, Phys. Rev. Lett. **120,** 193401 (2018).
[41] F. Engel, T. Dieterle, T. Schmid, C. Tomschitz, C. Veit, N. Zuber, R. Löw, T. Pfau, and F. Meinert, Phys. Rev. Lett. **121,** 193401 (2018).
[42] S. Haze, J. Wolf, M. Deiß, L. Wang, G. Raithel, and J. Hecker Denschlag, arXiv:1901.11069.